Laser and Particle Beams (2001), *19*, 253–257. Printed in the USA.

Angular distribution of X-ray line radiation from laser-irradiated planar targets

V. ARORA,[1] J.A. CHAKERA,[1] S.R. KUMBHARE,[1] P.A. NAIK,[1] N.K. GUPTA,[2] AND P.D. GUPTA[1]

[1]Plasma Radiation Section, Centre for Advanced Technology, Indore, 452013, India
[2]High Pressure Physics Division, Bhabha Atomic Research Centre, Mumbai, 400085, India

(RECEIVED 28 March 2000; ACCEPTED 9 December 2000)

Abstract

A study of angular distribution of X-ray line radiation emitted from a laser-produced plasma is presented. Plasma was produced by irradiating a planar magnesium target using single laser pulses of 6 J, 4.5 ns (FWHM) from an Nd:glass laser system. Angular distribution of X-ray emission in the spectral range of 7–10 Å was recorded using a single X-ray crystal spectrograph. X-ray emission intensity for different resonance lines is observed to decrease up to an angle of ~45° with respect to target normal, followed by a significant increase at higher angles. The observed departure of angular distribution from a monotonically decreasing behavior is broadly in agreement with the calculations of the escape factor of the radiation at different angles from a thick disk-shaped plasma using a spectroscopic code RATION.

Keywords: Angular distribution; Laser produced plasma; X-ray crystal spectrograph

1. INTRODUCTION

Study of intense soft X-ray emission from laser-produced plasmas is a subject of much current interest due to potential applications (Turcu & Dance, 1999) of this radiation in many areas, for example, indirect approach to laser-driven inertial confinement fusion (Lindl, 1995), pump source for soft X-ray lasers (Zhang & Fill, 1992; Li *et al.*, 1997), microscopic imaging of live biological specimen (Stead *et al.*, 1995), VLSI microlithography (Chaker *et al.*, 1992), X-ray diffraction (Rischel *et al.*, 1997), X-ray absorption spectroscopy (Nakano *et al.*, 1999), X-ray photoelectron spectroscopy (Kondo *et al.*, 1998) and so forth. While some studies are performed on spherical targets using multiple beam irradiation, a vast majority of laser–plasma interaction studies are carried out in plasmas produced from planar targets using a single laser beam. In addition to various applications, X-ray emission from such plasmas is often used for deriving information about plasma parameters such as density, temperature, ionization states, and so forth (Boiko, 1983; Hauer *et al.*, 1991). The X-ray emission from laser-irradiated planar targets is expected to show an anisotropic behavior due to variation in plasma opacity experienced by radiation emitted in different directions with respect to the target normal (Gupta & Kumar, 1995; Aglitskiy *et al.*, 1996). A knowledge of angular distribution of X-ray intensity is therefore necessary not only for a correct estimation of X-ray conversion efficiency, but in deriving plasma diagnostic information as well. Moreover, since X-ray emission intensity is governed by plasma hydrodynamics and the radiation transport involved, a study of angular distribution of X-ray emission can be helpful in understanding these processes in the plasma.

Several authors have reported on measurements of angular distribution of soft X-ray emission performed using X-ray diodes placed at discrete angles and filtered with suitable foils (Popil *et al.*, 1987; Broughton & Fedosejevs, 1993; Teubner *et al.*, 1995). Angular dependence of X-ray intensity in these studies was mostly fitted as some power law of $\cos\theta$, which is a monotonically decreasing function of the angle θ with respect to the target normal. It may be noted that most of these studies were carried out for X-ray emission integrated over a broad spectral range. A knowledge of angular intensity distribution of resonance line transitions is also desirable in view of various applications, for example, as a pump source for X-ray lasers (Hagelstein, 1983; Zhang & Fill, 1992) or in radiographic imaging of fusion targets (Matthews *et al.*, 1983; Brown *et al.*, 1997). However, the study of angular distribution of individual radiative line transitions are scarcely found in literature (Chase *et al.*, 1977). Since oscillator strength of line transitions is much larger as compared to that for the continuum radiation, the former are expected to show a more pronounced effect of

Address correspondence and reprint requests to: V. Arora, #209, R & D 'D' Block, Plasma Radiation Section, Centre for Advanced Technology, P.O. CAT, Indore, 452013, M.P., India. E-mail: pdgupta@cat.ernet.in

plasma opacity. Moreover, a study of angular distribution of resonance line emissions is desirable, as line intensity ratio is often used as a diagnostics means for plasma density and temperature.

In this article, we present a study of angular distribution of X-ray line radiation emitted from plasma produced from a planar magnesium target using 6 J, 4.5 ns Nd:glass laser pulses. The study was performed using a single planar crystal spectrograph with a provision of accounting for any variation in crystal reflectivity along its length. The observed behavior is found to be in agreement with that expected from a spectroscopic code RATION (Lee *et al.*, 1990) calculating the escape factor of the radiation at different angles from a thick disk-shaped plasma.

2. DESCRIPTION OF THE EXPERIMENT

The experiment was performed by irradiating a planar magnesium target using single laser pulses of 6 J, 4.5 ns (FWHM) from an Nd:glass laser system ($\lambda = 1.054\ \mu$m). Laser intensity on the target surface was $\sim 8 \times 10^{12}$ W/cm^2, corresponding to a focal spot diameter of $\sim 130\ \mu$m (determined from the half intensity points of the X-ray emission region). The X-ray emission spectrum was recorded by a crystal spectrograph specifically designed for this purpose. It consisted of a planar thallium acid phthalate crystal [TAP: $2d = 25.75$ Å (001) plane] of size $50 \times 25 \times 1$ mm (thickness) as a Bragg reflector. The target, crystal, and detector (X-ray film) were placed in a plasma chamber evacuated to 10^{-3} torr. Figure 1 illustrates the geometry of the spectrograph. X rays from the pointlike plasma source were reflected and spectrally dispersed at appropriate Bragg angles subtended at different points along the width of crystal (Fig. 1(a)). The angular intensity variation for a given wavelength was recorded from X rays incident at different points along the length of the crystal (Fig. 1(b)). The angular range is governed by the length of the crystal and its distance from the plasma source. The crystal was placed such that its center was at a distance of 35 mm from the plasma source. The angular range covered by 40 mm length of the crystal at this distance was $\sim 60°$. Thus complete distribution was recorded in two settings, ensuring considerable overlap of the two angular ranges.

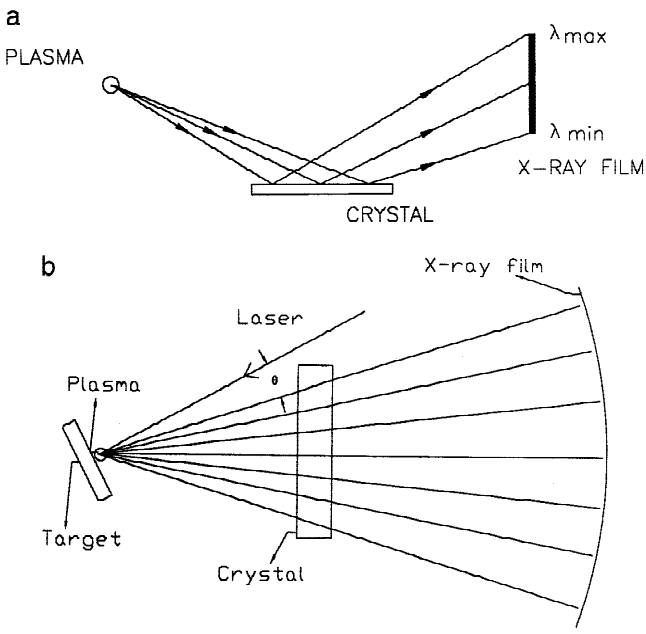

Fig. 1. Geometry of the crystal spectrograph operation: (a) X-ray reflection at different Bragg angles along the width of the crystal results in dispersion. (b) Angular distribution is obtained by recording X rays emitted at different angles with respect to target normal, and reflected from different points along the length of the crystal.

The X-ray spectrograph was positioned so as to cover a range of Bragg angles from 15° to 23°. This corresponds to an X-ray spectral range of 7–10 Å, which covers most of the important transitions in He-like and H-like ions of magnesium plasma. The spectrum was recorded on a DEF-5 X-ray film, which was mounted concentric with the plasma source at a distance of 77 mm. The X-ray film was covered with two thin aluminized polycarbonate foils to protect it from exposure to any scattered visible, UV, and XUV radiations. The cutoff energy (corresponding to $1/e$ transmission) of the two foils was ~ 0.9 keV. The exposed film was developed for a period of 5 min in D-19 developer with a standard procedure. The dispersion of the film plane was 0.33 Å/mm (at $\lambda = 917$ Å) and spectral resolution was ~ 45 mÅ.

In principle, the angular distribution of X-ray intensity recorded on the detector may be somewhat different from the actual angular distribution due to possible variation in the crystal reflectivity along its length. Therefore, a correction factor for the same was experimentally determined by increasing the distance of the crystal from the plasma source to 221 mm. In this setting, the crystal length covered only a smaller angular range of $\sim 10°$ of X-ray emission from the source, for which anisotropy in the X-ray intensity is expected to be small. The angular variation of the X-ray intensity for a given spectral line in this case would be essentially due to variation in the crystal reflectivity. This variation was observed to be within $\pm 15\%$ from one end of the crystal to the other end. This variation was used to derive the actual angular distribution of X-ray intensity from the data recorded with the crystal placed at distance of 35 mm. In order to ascertain that the angular distribution thus obtained does not contain the effect of instrumental anisotropy, the experiment was repeated by reversing the crystal about its length, that is, the two ends of the crystal looking at lower and higher angles, respectively, were reversed. The two sets of data derived after making correction for variation in the crystal reflectivity were observed to be about the same.

3. RESULTS AND DISCUSSION

Figure 2 shows a densitometric trace of a single-shot X-ray emission spectrum of magnesium plasma observed at an

https://doi.org/10.1017/S0263034601192153 Published online by Cambridge University Press

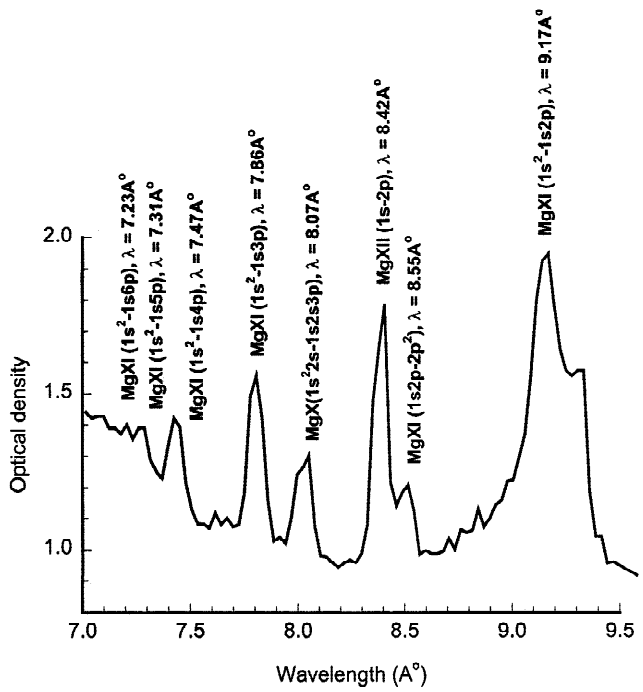

Fig. 2. A densitometric trace of X-ray emission spectrum of magnesium plasma observed from at an angle of 15° from the target normal.

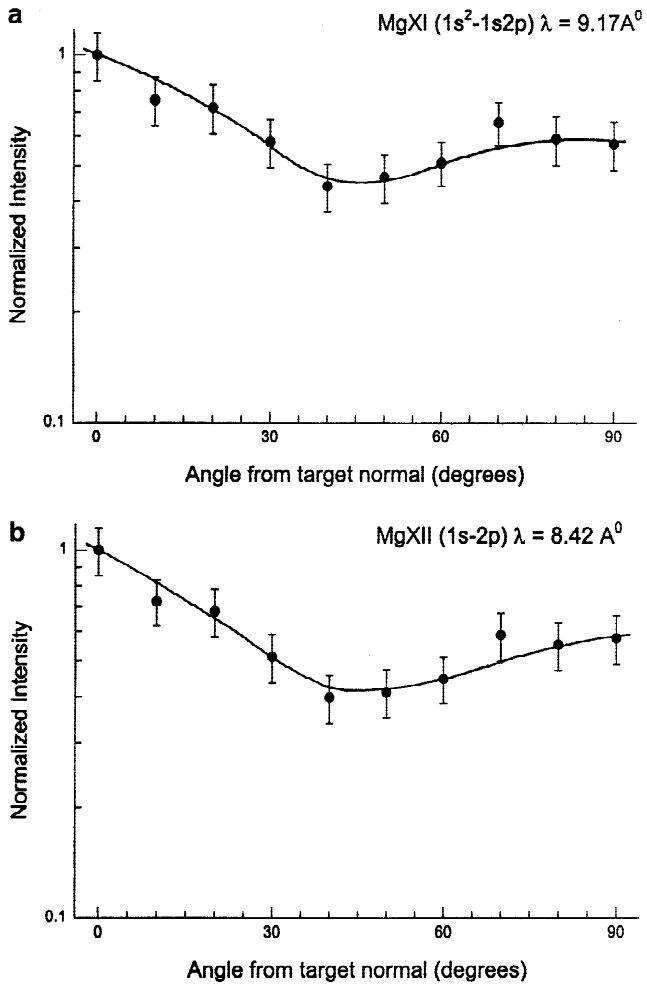

Fig. 3. Variation of intensity of X-ray line radiation with respect to the angle from the target normal: (a) Mg XI ($1s^2$–$1s\,2p$) $\lambda = 9.17$ Å, (b) Mg XII ($1s$–$2p$) $\lambda = 8.42$ Å.

angle of 15° from the target normal. Optical density of the recorded spectrum was determined by using a densitometer (Model Carl-Zeiss). Various prominent lines in the spectrum are identified as transitions in Li-like, He-like, and H-like magnesium ions, namely, MgXI ($1s^2$–$1s2p$) $\lambda = 9.17$ Å, MgXI ($1s2p$–$2p^2$) $\lambda = 8.55$ Å, MgXII ($1s$–$2p$) $\lambda = 8.42$ Å, MgXI ($1s^2$–$1s3p$) $\lambda = 7.86$ Å, MgX ($1s^2 2s$–$1s2s3p$) $\lambda = 8.07$ Å, MgXI ($1s^2$–$1s4p$) $\lambda = 7.47$ Å, MgXI ($1s^2$–$1s5p$) $\lambda = 7.31$ Å, MgXI ($1s^2$–$1s6p$) $\lambda = 7.23$ Å. Spectral intensity distribution was obtained from the densitometric trace by using the measured relative response of the film, that is, optical density versus exposure. The latter was obtained using the step filter technique under the same developing procedure.

Angular distribution for the two most intense resonance lines, namely, MgXI ($1s^2$–$1s2p$) $\lambda = 9.17$ Å and MgXII ($1s$–$2p$) $\lambda = 8.42$ Å is shown in Figures 3(a) and 3(b), respectively. In both figures, the angular distribution shows a significant departure from a monotonically decreasing behavior. It is seen that for both line transitions, the X-ray intensity first decreases with an angle up to ~45°, and then shows an increase for higher angles. The curves shown in the two figures are drawn only to guide the eye. The ratio of X-ray intensity at ~45° to that in the direction of target normal is ~0.45 for MgXI ($1s^2$–$1s2p$) $\lambda = 9.17$ Å, and ~0.4 for MgXII ($1s$–$2p$) $\lambda = 8.42$ Å. The intensity increases for angles larger than ~45°, and reaches a value at an angle ~80° to 90° of about 0.7 times that in the direction of the target normal.

Anisotropy of X-ray emission can be understood to be due to the effect of plasma opacity. Angular distribution of radiation intensity at particular frequency, from a plasma of certain volume and shape containing a given number of emitters, would be governed by the escape factor ($\exp -\tau$) faced by the radiation in traversing the plasma in different directions. For an optically thin plasma (i.e., $\tau \ll 1$), the escape factor is nearly equal to unity for all directions. In this case, the angular distribution is expected to be isotropic. On the other hand, if the plasma is not optically thin, the escape factor may be different for different directions. For a coin-shaped plasma, the escape factor in the direction of target normal is highest because the smallest plasma thickness is encountered in that direction. The escape factor decreases with increasing angle from target normal as the plasma thickness increases. Anisotropic X-ray emission from plasma produced from planar targets exhibiting power law of the form $\cos^{\alpha}\theta$ (Popil *et al.*, 1987; Broughton & Fedosejevs, 1993; Teubner *et al.*, 1995) is consistent with these considerations.

https://doi.org/10.1017/S0263034601192153 Published online by Cambridge University Press

A quantitative knowledge of the effect of opacity variation on angular distribution would require use of sophisticated computer simulations based on plasma hydrodynamic codes including radiation transport (Ramis *et al.*, 1988). Nevertheless, some important features can be realized by approximating the plasma to be of some geometrical shape, and making certain simplifying assumptions on the spatial variations of plasma density and temperature. For example, in a coin-shaped uniform plasma, where thickness of the plasma (along the direction of target normal) is much smaller than its diameter, the distance traversed by radiation in escaping from the plasma will be minimum along the target normal, and the same will increase with increase in angle θ. As a result, the X-ray intensity will show a monotonically decreasing angular distribution of the form $\cos^{\alpha}\theta$ where α is an exponent depending on the plasma opacity. Chase *et al.* (1977) have explained their results showing a monotonically decreasing angular distribution of X-ray intensity of resonance line emission from a planar aluminum target by considering a coin-shaped plasma. This is reasonably justified, as the plasma in their experiment was produced by a short duration laser pulse of 200 ps. The plasma expansion length along the target normal during the laser pulse was therefore much smaller than the focal spot diameter.

The angular distribution observed in our experiment (Figs. 3(a) and 3(b)) shows departure from monotonically decreasing behavior for $\theta > 45°$, and this cannot be explained by considering a coin-shaped planar geometry. However, this behavior can be understood by realizing that for the longer laser pulse of 4.5 ns (FWHM) used in the present study, plasma expansion geometry would be quite different. In laser-irradiated planar targets with a finite-size focal spot, the plasma expansion may be considered to be nearly planar to an expansion distance d of the order of focal spot radius r_0 as schematically represented in Figure 4. The plasma expansion time to reach this position is $t_{exp} \approx r_0/c_s$ where c_s is the plasma sound speed. For $t_L \ll t_{exp}$, the plasma expansion would remain nearly planar and its expansion distance will be much smaller than r_0. In this case, plasma can be approximated to be of a coin-shaped geometry. However, for pulse duration $t_L \gg t_{exp}$, the plasma expansion reaches a steady-state profile. In this case, the plasma may be considered to consist of two regions: first a planar expansion region of high density for $d \leq r_0$, and the second one being a spherically expanding region for $d > r_0$ with a fast decreasing density (Mora, 1982). In our experiment, the electron temperature and electron density of the plasma, determined from the ratio of X-ray line intensities, was 275 ± 50 eV and $(3.5 \pm 1) \times 10^{20}$/c.c., respectively. Using the corresponding sound speed c_s of 1.5×10^7 cm/s, the expansion time will be ~0.4 ns for $r_0 = 65$ μm. Since laser pulse duration t_L of 4.5 ns is much larger than this value, a steady-state description of the plasma expansion profile should be applicable in the present case.

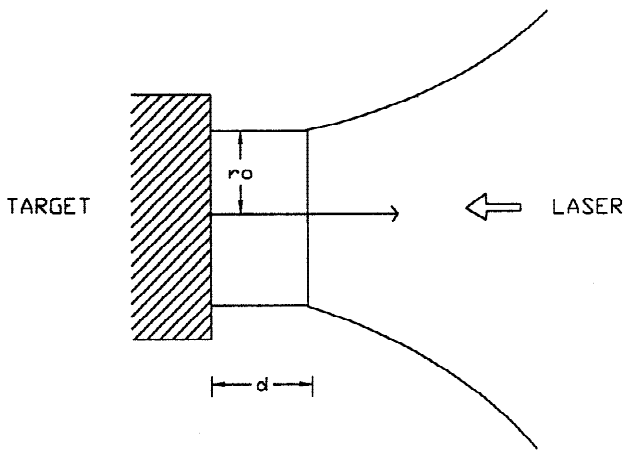

Fig. 4. A schematic representation of the plasma expansion geometry.

The observed behavior of the angular distribution of X-ray intensity can now be explained by considering the escape factor experienced by radiation emitted in different directions from the plasma of the above described geometry. The planar expansion region, due to its high density as well as high temperature, makes the largest contribution to the emitted radiation. It may be seen from Figure 4 that the physical length of the plasma encountered by radiation to escape from this region would increase from $\theta = 0$ up to an angle $\tan^{-1}(d/r_0)$, and then decrease for higher values of θ. Since $d \sim r_0$ for the plasma expansion geometry shown in Figure 4, one would observe a minimum in angular distribution for $\theta \sim 45°$. Further, in principle, one should expect an increase in half width of the spectral line with an increase in optical thickness. However, such a variation could not be observed because the line width of ~45 mÅ, which is essentially governed by the source size, would mask the effect of any opacity broadening.

Optical depth for radiative line transitions can be calculated for a specified plasma size using spectroscopic code RATION (Lee *et al.*, 1990). An idea of the escape factor of radiation coming out of the plasma can be obtained by using this code and taking the distance travelled by radiation in different directions to be $r_0/\cos\theta$. Escape factor of radiation using the RATION code and taking electron temperature of 300 eV and electron density of 3.5×10^{20}/c.c. is shown in Figure 5 for the two line transitions MgXI ($1s$–$2p$) and MgXII ($1s^2$–$1s2p$). It is seen that the escape factor decreases up to an angle ~45° and then increases for higher angles, a behavior similar to that noted from the measured angular distribution of the X-ray emission. In principle, the angular distribution would be a summation of the X-ray intensity emitted from different points in the plasma using corresponding values of escape factor. An exact calculation of the same would require detailed temperature and density profiles of the plasma and would be a quite complicated task. Nevertheless, the typical variation of the escape factor with angle (Fig. 5) reasonably well explains the qualitative features of the observed angular distribution of X-ray emission with a broad quantitative agreement.

https://doi.org/10.1017/S0263034601192153 Published online by Cambridge University Press

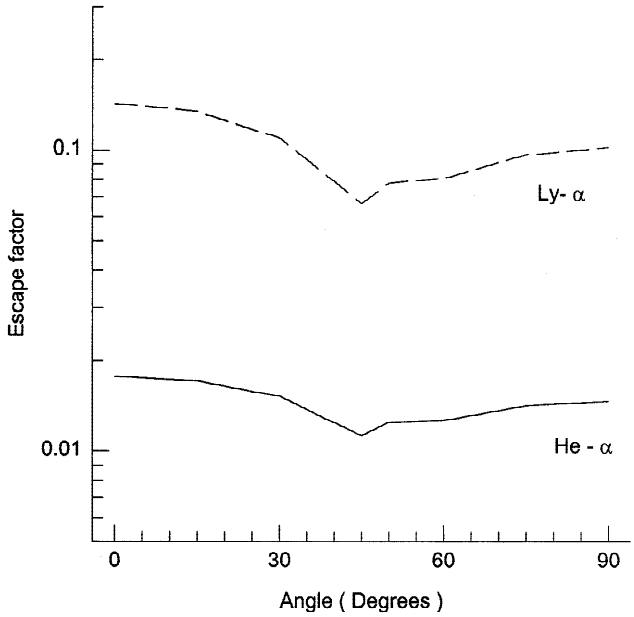

Fig. 5. Computed values of the escape factor of MgXII ($1s$–$2p$) and MgXI ($1s^2$–$1s2p$) for different angles with respect to the target normal.

In conclusion, we have presented a study of angular distribution of X-ray line radiation from a laser-irradiated planar magnesium target. Departure from monotonically decreasing angular distribution is consistent with calculations of the escape factor of the radiation from a broad disk-shaped plasma which comes as a result of the role of plasma hydrodynamics in the long pulse regime.

REFERENCES

Aglitskiy, Y., Lehecka, T., Deniz, A., Hardgrove, J., Seely, J., Brown, C., Feldman, U., Pawley, C., Gerber, K., Bodner, S., Obenschain, S., Lehmberg, R., Mclean, E., Pronko, M., Sethian, J., Stamper, J., Schmitt, A., Sullivan, C., Holland, G. & Laming, M. (1996). X-ray emission from plasmas created by smoothed krF laser irradiation. *Phys. Plasmas* **3**, 3438–3447.

Boiko, V.A. (1983). The determination of parameters of recombining laser produced plasmas by means of X-ray spectroscopy. *J. Phys. B* **16**, L77–L81.

Broughton, J.N. & Fedosejevs, R. (1993). keV X-ray production using 50 mJ krF laser-produced plasma. *J. Appl. Phys.* **74**, 3712–3723.

Brown, C., Seely, J., Feldman, U., Obenschain, S., Bodner, S., Pawley, C., Gerber, K., Sethian, J., Mostovych, A., Aglitskiy, Y., Lehecka, T. & Holland, G. (1997). High resolution X-ray imaging of planar foils irradiated by the Nike krF laser. *Phys. Plasmas* **4**, 1397–1401.

Chaker, M., Fontaine, B.La, Cote, C.Y., Kieffer, J.C., Pepin, H., Talon, M.H., Enright, G.D. & Villeneuve, D.M. (1992). Laser plasma sources for proximity printing or projection X-ray lithography. *J. Vac. Sci. Technol.* **B10**, 3239–3242.

Chase, L.F., Jordon, W.C., Perez, J.D. & Pronko, J.G. (1977). Angular distributions of X-ray line radiation from laser produced plasma. *Appl. Phys. Lett.* **30**, 137–139.

Gupta, N.K. & Kumar, V. (1995). Angular dependence of M and N band radiation and the effect of angular anisotropy on the total conversion efficiency of X-ray emitted from a laser irradiated gold foil. *Laser Part. Beam* **13**, 389–402.

Hagelstein, P.L. (1983). Review of radiation pumped soft X-ray lasers. *Plasma Phys.* **25**, 1345–1367.

Hauer, A.A., Delamater, N.D. & Koenig, Z.M. (1991). High resolution X-ray spectroscopic diagnostics of laser heated and ICF plasmas. *Laser Part. Beams* **9**, 3–48.

Kondo, H., Tomio, T. & Shimizu, H. (1998). Observation of chemical shifts of Si 2*p* level by an X-ray photoelectron spectroscopy system with a laser plasma X-ray source. *Appl. Phys. Lett.* **72**, 2668–2670.

Lee, R.W., Strout, R.E., Cauble, R.C. & Petway, L.B. (1990). *RATION spectroscopic code,* Lawrence Livermore National Laboratory, USA.

Li, Y., Schillinger, H., Ziener, C. & Sauerbrey, R. (1997). Reinvestigation of the Duguay soft X-ray laser: A new parameter space for high power femtosecond laser pumped systems. *Opt. Commun.* **144**, 118–124.

Lindl, J. (1995). Development of the indirect drive approach to inertial confinement fusion and the target physics basis for ignition and gain. *Phys. Plasmas* **2**, 3933–4000.

Matthews, D.L., Campbell, E.M., Ceglio, N.M., Hermes, G., Kauffman, R., Koppel, L., Ley, R., Manes, K., Rupert, V., Slivinsky, V.W., Turner, R. & Ze, F. (1983). Characterization of laser produced plasma X-ray source for use in X-ray radiography. *J. Appl. Phys.* **54**, 4260–4268.

Mora, P. (1982). Theoretical model of absorption of laser light by a plasma. *Phys. Fluids* **25**, 1051–1056.

Nakano, H., Goto, Y., Lu, P., Nishikawa, T. & Uesugi, N. (1999). Time resolved soft X-ray absorption spectroscopy of silicon using femtosecond laser plasma X-rays. *Appl. Phys. Lett.* **75**, 2350–2352.

Popil, R., Gupta, P.D., Fedosejevs, R. & Offenberger, A.A. (1987). Measurement of krF laser plasma X-ray radiation from targets with various atomic numbers. *Phys. Rev. A* **35**, 3874–3882.

Ramis, R., Schmalz, R. & Meyer-ter-vehn, J. (1988). Multi—a computer code for one-dimensional multigroup radiation hydrodynamics. *Comput. Phys. Commun.* **49**, 475–505.

Rischel, C., Rousse, A., Uschmann, I., Albouy, P.A., Geindre, J.P., Audebert, P., Gauthier, J.C., Forster, E., Martin, J.L. & Antonetti, A. (1997). Femtosecond time resolved X-ray diffraction from laser heated organic films. *Nature* **390**, 490–492.

Stead, A.D., Cotton, R.A., Duckett, J.G., Goode, J.A., Page, A.M. & Ford, T.W. (1995). The use of soft X-rays to study the ultra structure of living biological material. *J. X-ray Sci. Technol.* **5**, 52–64.

Teubner, U., Wulker, C., Theobald, W., Forster, E. (1995). X-ray spectra from high intensity subpicosecond laser produced plasmas. *Phys. Plasmas* **2**, 972–981.

Turca, I.C.E. & Dance, J.B. (1999). *X-rays from laser plasmas.* New York: John Wiley and Sons.

Zhang, J. & Fill, E. (1992). Resonantly photo pumped Fe^{16+} soft X-ray laser. *Optical Quantum Electron.* **24**, 1343–1350.

https://doi.org/10.1017/S0263034601192153 Published online by Cambridge University Press